Acta Crystallographica Section D
Biological Crystallography
ISSN 0907-4449

Preliminary structure analysis of the DH/PH domains of leukemia-associated RhoGEF

Romana Kristelly,[a] Brett T. Earnest,[a] Lakshmipriya Krishnamoorthy[b] and John J. G. Tesmer[b]*

[a]Department of Chemistry and Biochemistry, The University of Texas at Austin, Austin, TX 78712, USA, and [b]Institute for Cellular and Molecular Biology, The University of Texas at Austin, Austin, TX 78712, USA

Correspondence e-mail: tesmer@mail.utexas.edu

Received 24 July 2003
Accepted 13 August 2003

Leukemia-associated RhoGEF (LARG) is a multidomain protein that relays signals from $G\alpha_{12/13}$-coupled heptahelical receptors to GTPases that regulate the cytoskeleton. To understand the molecular basis of LARG-mediated signal transduction, structural analysis of its DH/PH domains has been initiated. The LARG DH/PH domains have been overexpressed in *Escherichia coli* as a TEV protease-cleavable fusion protein containing maltose-binding protein and a hexahistidine tag at the N- and C-termini, respectively. Crystals of the DH/PH domains were obtained (space group *C*2; unit-cell parameters $a = 195.5$, $b = 46.0$, $c = 75.1$ Å, $\beta = 105.0^\circ$) and xenon and NaBr derivatives were generated which should allow the structure to be determined by MIRAS.

1. Introduction

Leukemia-associated RhoGEF (LARG) belongs to a subfamily of Rho guanine-nucleotide exchange factors (RhoGEFs) that are involved in signalling from G protein-coupled receptors (GPCRs) to Rho GTPases and thus to the cytoskeleton (Schmidt & Hall, 2002). This family of RhoGEFs, which also includes PDZ-RhoGEF/GTRAP48 and p115RhoGEF/Lsc, is characterized by a regulator of G protein signalling homology (RH) domain positioned N-terminal to Dbl and pleckstrin homology (DH/PH) tandem domains. RhoGEFs activate Rho GTPases by catalyzing the transformation of their inactive (GDP-bound) to their active (GTP-bound) form. Unlike other structurally characterized RhoGEFs, the RH-domain-containing RhoGEFs (RH-RhoGEFs) are specific for the Rho subfamily of Rho GTPases. Structures of DH/PH domains from Tiam1 (Worthylake *et al.*, 2000), intersectin (Snyder *et al.*, 2002) and Dbs (Rossman *et al.*, 2002) in complex with Rac1 and Cdc42 have demonstrated that the catalytic residues essential for nucleotide exchange reside within the DH domain. For most RhoGEFs, the role of the PH domain in GTPase activation is not clear.

In vitro nucleotide-exchange experiments show that the DH domain of LARG has less GEF activity than its DH/PH domains (Reuther *et al.*, 2001). A similar phenomenon was observed with p115RhoGEF (Wells *et al.*, 2001). This suggests that the LARG PH domain contributes to substrate binding and catalysis. Contacts between the PH domain of a RhoGEF with its substrate have only previously been observed in the Dbs–Cdc42 (Rossman *et al.*, 2002) and Dbs–RhoA structures (Snyder *et al.*, 2002). These structures revealed that several residues from the PH domain interact directly with the GTPase. However, these residues are not conserved in the RH-RhoGEF family. A structure of the DH/PH domains of LARG might therefore reveal a novel mechanism of PH domain-assisted nucleotide exchange.

LARG is regulated at least in part through its RH domain, which has been shown to interact with $G\alpha$ subunits of the $G\alpha_{12/13}$ family (Fukuhara *et al.*, 2000). LARG and other RH-RhoGEFs therefore represent a direct link between transforming GPCRs and small GTPases (Fukuhara *et al.*, 2001). *In vitro* experiments with p115RhoGEF show that association with $G\alpha_{13}$ increases the nucleotide-exchange activity of the RhoGEF (Hart *et al.*, 1998). Further experiments suggested that an additional binding site for $G\alpha_{13}$ is found within the DH/PH domains (Wells *et al.*, 2002). However, the mechanism of $G\alpha$-mediated activation remains unclear.

The structure of the DH/PH domains of LARG will reveal features specific to DH/PH domains of the RH-RhoGEF family. In particular, it may identify binding sites for $G\alpha_{12/13}$ family proteins and elucidate the molecular determinants for exclusive recognition of RhoA.

2. Methods

2.1. Cloning, expression and purification of the DH/PH domains of LARG

A fragment of human LARG encoding the DH/PH domains (residues 765–1138) was inserted into a modified pMALc2X vector (New England Biolabs) using *Bam*HI and *Sal*I restriction sites. The modified vector (pMALc2T-H_6) was generated by replacing the

factor Xa protease recognition site with that of tobacco etch virus (TEV) protease and inserting a sequence that encodes a C-terminal hexahistidine (H_6) tag followed by a stop codon. The pMALc2X vector was first digested with restriction enzymes *Ava*I and *Bam*HI. 5′-phosphorylated oligonucleotides encoding the TEV protease recognition site (tcggggaaaacctgtattttccagg and gatccctgaaaatacaggttttcc; Integrated DNA Technologies) were mixed in equimolar amounts, heated to 353 K for 10 min, allowed to cool and ligated with the digested pMALc2X vector using T4 DNA ligase (Sigma). To insert the sequence for the C-terminal H_6 tag, the vector was then digested with the restriction enzymes *Sal*I and *Hin*dIII and complementary oligonucleotides (tcgacggaggtcaccaccaccaccaccactaaa and agcttttagaggaggaggaggaggagacctccg; Integrated DNA Technologies) were inserted as described above. The DH/PH domains expressed from this vector are thus fusion proteins that have maltose-binding protein (MBP) at the N-terminus and an H_6 tag at the C-terminus. After treatment with TEV protease, the H_6-tagged DH/PH domains have a molecular weight of 44.7 kDa.

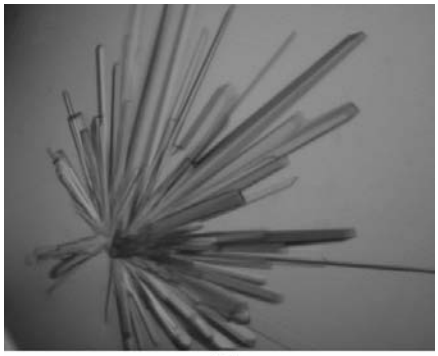

(*a*)

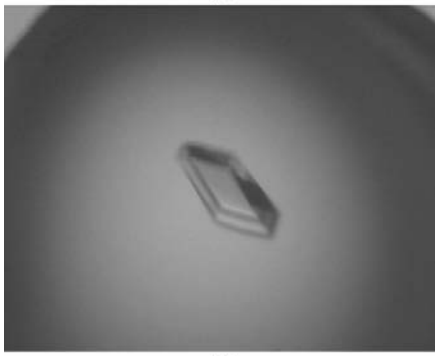

(*b*)

Figure 1
Crystals of the DH/PH domains of human leukemia-associated RhoGEF (LARG). (*a*) Initial crystals grown as needle clusters (approximate dimensions 0.2 × 0.02 × 0.02 mm). (*b*) A single crystal grown under optimized conditions (approximate dimensions 0.4 × 0.2 × 0.05 mm).

The DH/PH-domain fragment of LARG was expressed using *Escherichia coli* strain Rosetta (DE3) pLysS (Novagen). Cells were grown in Luria–Bertani media supplemented with 0.2% α-D-glucose, 50 μg ml^{-1} carbenicillin and 34 μg ml^{-1} chloramphenicol at 310 K to an OD_{600} of 0.6. Protein expression was induced with 100 μ*M* isopropylthiogalactopyranoside at 310 K and cells were harvested after 24 h by centrifugation for 10 min at 3500 rev min^{-1} in a Beckman Coulter Avanti J-20 centrifuge using a JLA 8.100 rotor. The cell pellet was frozen in liquid nitrogen and stored at 193 K until purification.

Cells were lysed with lysozyme (1 mg ml^{-1}; Sigma) in lysis buffer [20 m*M* HEPES pH 8.0, 300 m*M* NaCl, 10 m*M* β-mercaptoethanol (β*M*E), 10 m*M* imidazole pH 8.0] supplemented with 0.3 m*M* EDTA and protease inhibitors (1 μ*M* leupeptin, 1 m*M* lima bean trypsin inhibitor, 1 m*M* PMSF and 1 m*M* TPCK). Lysates were treated with 20 μg DNaseI (Sigma) per gram of *E. coli* and centrifuged for 45 min at 35 000 rev min^{-1} in a Beckman Coulter Optima LE-80K ultracentrifuge, using a type 45 Ti rotor. The supernatant was then loaded onto a drip column containing immobilized nickel resin (Ni–NTA Superflow, Qiagen) pre-equilibrated with lysis buffer. After washing with five column volumes of lysis buffer and five column volumes of wash buffer (lysis buffer containing 20 m*M* imidazole), protein was eluted in 1 ml fractions with elution buffer (lysis buffer containing 250 m*M* imidazole). Fractions containing the MBP-DH/PH fusion protein were pooled and dialyzed overnight against dialysis buffer (20 m*M* HEPES pH 8.0, 300 m*M* NaCl, 5 m*M* β*M*E) in the presence of 1.5%(*w*/*w*) TEV protease. Afterwards, the DH/PH domains were separated from cleaved MBP by nickel-affinity chromatography as described above for the fusion protein. Finally, fractions containing the DH/PH domains were pooled, concentrated and loaded onto a size-exclusion chromatography column (Superdex 200 16/60, Amersham Pharmacia Biotech) pre-equilibrated with gel-filtration buffer (20 m*M* HEPES pH 8.0, 100 m*M* NaCl, 1 m*M* DTT). Fractions containing the DH/PH domains were pooled, concentrated to approximately 10 mg ml^{-1} and stored at 193 K. The typical yield is of pure protein is 15 mg per litre of cell culture.

TEV protease was expressed from the pRK793 expression vector (Kapust *et al.*, 2001). Lysis was performed as described above for the DH/PH domains using TEV-lysis buffer (20 m*M* HEPES pH 8.0, 100 m*M* NaCl, 25 m*M* imidazole pH 8.0, 10 m*M* β*M*E, 10% glycerol). The lysate was loaded onto an Ni–NTA column (Qiagen) that was pre-equilibrated with TEV-lysis buffer. The column was then washed with ten column volumes of TEV-lysis buffer and TEV protease was eluted in 1 ml fractions with TEV-elution buffer (TEV-lysis buffer containing 250 m*M* imidazole pH 8.0). Fractions containing TEV protease were pooled, concentrated to 1 mg ml^{-1} and loaded onto a size-exclusion chromatography column (Superdex 200 16/60, Amersham Pharmacia Biotech), which was pre-equilibrated with TEV gel-filtration buffer (20 m*M* HEPES pH 8.0, 200 m*M* NaCl, 2 m*M* EDTA, 10 m*M* DTT, 10% glycerol). Fractions containing TEV protease were pooled, concentrated to approximately 1 mg ml^{-1} and stored at 193 K.

2.2. Crystallization

Crystals (Fig. 1) were obtained by the hanging-drop method from drops containing 1 μl of the concentrated protein and 1 μl of a well solution suspended over 1 ml of the well solution. Initial crystallization trials employed both a commercial screen (Crystal Screen Lite, Hampton Research) and a set of screens developed in-house that vary the concentration of PEG (molecular weights 400, 3350, 8000 and 10 000) or salt (ammonium sulfate or NaCl) against various buffers in the pH range 5.0–8.0 in steps of 0.5 pH units. The PEG screens were performed at both low and high ionic strength (100 m*M* and 1 *M* NaCl, respectively). Needle clusters (Fig. 1*a*) appeared in one of the in-house screens at 15% PEG 3350, 1 *M* NaCl and 100 m*M* sodium citrate pH 6.5. Upon optimization of the pH, NaCl and PEG concentrations, single crystals (Fig. 1*b*) were grown at 277 K in 8–11% PEG 3350, 0.8–1.1 *M* NaCl and 100 m*M* sodium citrate pH 6.5. Nucleation occurs within 3 d and crystals reach their maximum size in approximately two weeks. Crystals belong to space group *C*2 and have unit-cell parameters a = 195.5, b = 46.0, c = 75.1 Å, β = 105.0°. There could be either one or two monomers per asymmetric unit (V_M = 3.5 and 1.8 Å^3 Da^{-1}, respectively). The crystals must be harvested within several weeks of growth to avoid gradually increasing the mosaicity and loss of resolution.

2.3. X-ray diffraction data collection and processing

Native crystals were harvested by gradual addition of 1 μl cryoprotectant solution

(20% PEG 3350, 15% ethylene glycol, 1 *M* sodium chloride, 100 m*M* sodium citrate pH 6.5) at a time to the hanging drop and subsequently transferring crystals to the cryoprotectant solution using cryoloops (Hampton Research). Cryoprotected crystals were flash-frozen in liquid nitrogen and a native data set was collected using a Quantum 4 CCD detector (ADSC) at the Advanced Photon Source beamline 14D (BioCARS) (Table 1). The crystal was maintained at 90 K throughout data collection. Data were reduced and scaled using the *HKL* package (Otwinowski & Minor, 1997). Because molecular replacement with the program *MOLREP* (Vagin & Teplyakov, 1997) using either the DH/PH or DH domains of related RhoGEFs failed, we produced xenon and sodium bromide derivatives in order to obtain an initial set of phases. The xenon derivative was generated by subjecting a crystal to 3.6 MPa xenon in a xenon chamber (Hampton Research) for 30 min at 277 K and the bromide derivative by soaking crystals in cryoprotectant solution for 48 h with NaBr substituting for NaCl. Diffraction intensities from both derivatives were collected using Cu $K\alpha$ radiation on a MAR345 imaging-plate detector (Table 1). The temperature was maintained at 95 K with an Oxford Instruments Cryojet. Data were reduced and scaled using the *HKL*2000 package and isomorphous and anomalous difference Patterson maps were generated with programs from the *CCP*4 suite (Collaborative Computational Project, Number 4, 1994). The xenon derivative generated interpretable isomorphous and anomalous difference Patterson maps (Fig. 2). The first two xenon sites in these maps were identified by inspection and a remaining weaker site was found after refinement using *MLPHARE* (Otwinowski, 1991) and inspection of difference Fourier maps. The NaBr derivative had only one site, which was identified in difference Fourier maps generated using the xenon-derived phases. Preliminary electron-density maps suggest that the MIRAS phases from these two derivatives will be sufficient to ultimately allow the structure determination of the LARG DH/PH domains.

Table 1
Data-collection and MIRAS statistics of native and derivative crystals of the LARG DH/PH domains.

Values in parentheses refer to the highest resolution shell (native, 2.12–2.05 Å; xenon derivative, 3.62–3.5 Å; NaBr derivative, 2.49–2.4 Å).

	Native	Derivatives	
		Xenon	NaBr
Wavelength (Å)	0.9794	1.5418	1.5418
Space group	*C*2	*C*2	*C*2
Unit-cell parameters			
a (Å)	195.5	194.4	194.1
b (Å)	46.0	46.1	45.9
c (Å)	75.13	75.0	74.8
β (°)	105.0	104.5	106.6
Resolution (Å)	2.05	3.5	2.4
Unique reflections	41093	8384	25235
Total reflections	518961	67240	120925
Completeness (%)	96.8 (97.8)	100 (100)	99.8 (100)
R_{sym}† (%)	4.8 (51.4)	7.9 (16.1)	6.2 (42.3)
Average $I/\sigma(I)$	24.0 (3.1)	28.6 (12.6)	32.2 (4.8)
Phasing power‡			
Centric	—	0.98	0.19
Acentric	—	1.19	0.26
R_{cullis}§ (iso/ano)	—	0.74/0.96	0.98/1.0

† $R_{sym} = \sum |I - I_{avg}| / \sum I$, where the summation is over all symmetry-equivalent reflections, excluding reflections observed only once. ‡ Phasing power = (F_H/LOC), where LOC is the lack of closure. § $R_{cullis} = \big||F_{PH} \pm F_P| - F_H\big| / |F_{PH} - F_P|$ for centric reflections.

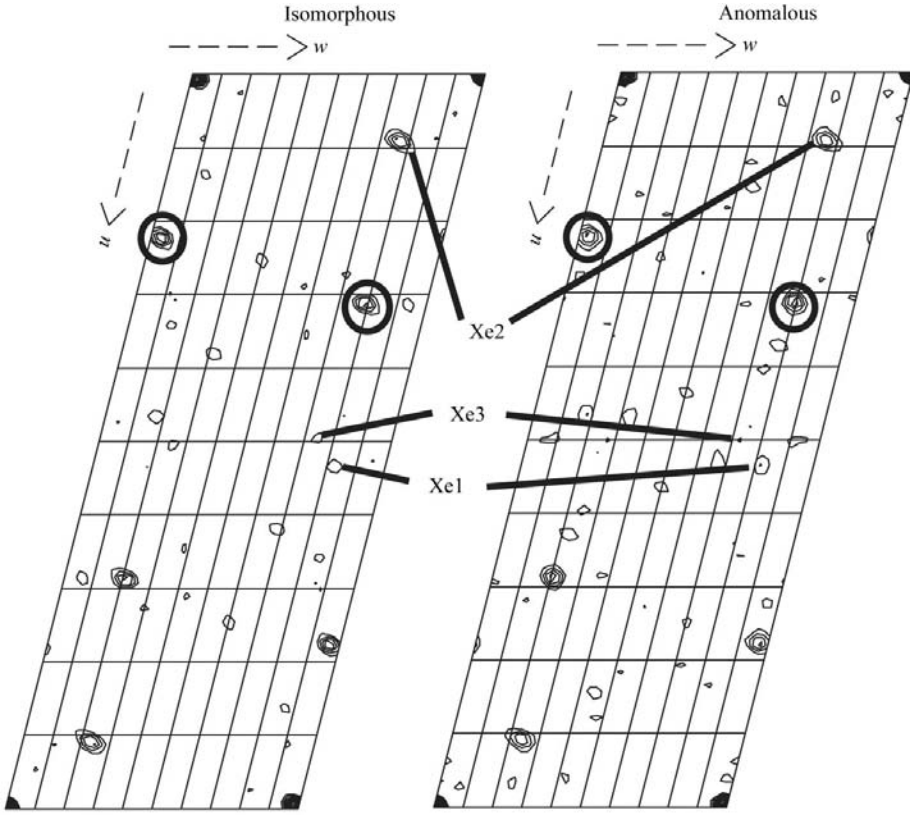

Figure 2
Harker section ($v = 0$) of isomorphous and anomalous difference Patterson maps of the LARG xenon derivative contoured starting at 1.0σ in steps of 1.0σ. One unit cell is shown. The three xenon Harker peaks are indicated (Xe1–Xe3). Circles indicate cross-peaks between two sets of symmetry-related xenon sites (Xe1 and Xe2) which also happen to occur on the Harker section.

We thank Dr Tohru Kozasa (University of Illinois at Chicago Medical Center) for providing us with the cDNA plasmid for LARG, as well as Dr David Waugh (NCI) for providing the TEV-protease expression vector. We thank the staff at the BioCARS beamline 14-BMD at the Advance Photon Source (APS) for their help with data collection. Furthermore, we would like to acknowledge Maria Pham for assistance with cloning of the modified pMALc2X plasmids. This work was supported by Welch Foundation chemical research grant F-1487 and American Heart Association Scientist Development Grant 0235273N (JJGT). Use of the APS was supported by the US Department of Energy, Basic Energy

Sciences, Office of Science under Contract No. W-31-109-Eng-38. Use of the BioCARS Sector 14 was supported by the National Institutes of Health, National Center for Research Resources under grant number RR07707.

References

Collaborative Computational Project, Number 4 (1994). *Acta Cryst.* D**50**, 760–763.
Fukuhara, S., Chikumi, H. & Gutkind, J. S. (2000). *FEBS Lett.* **485**, 183–188.
Fukuhara, S., Chikumi, H. & Gutkind, J. S. (2001). *Oncogene*, **20**, 1661–1668.
Hart, M. J., Jiang, X., Kozasa, T., Roscoe, W., Singer, W. D., Gilman, A. G., Sternweis, P. C. & Bollag, G. (1998). *Science*, **280**, 2112–2114.
Kapust, R. B., Tèozsâer, J., Fox, J. D., Anderson, D. E., Cherry, S., Copeland, T. D. & Waugh, D. S. (2001). *Protein Eng.* **14**, 993–1000.
Otwinowski, Z. (1991). *Proceedings of the CCP4 Study Weekend. Isomorphous Replacement and Anomalous Scattering*, edited by W. Wolf, P. R. Evans & A. G. W. Leslie, pp. 80–86. Warrington: Daresbury Laboratory.
Otwinowski, Z. & Minor, V. (1997). *Methods Enzymol.* **276**, 307–326.
Reuther, G. W., Lambert, Q. T., Booden, M. A., Wennerberg, K., Becknell, B., Marcucci, G., Sondek, J., Caligiuri, M. A. & Der, C. J. (2001). *J. Biol. Chem.* **276**, 27145–27151.
Rossman, K. L., Worthylake, D. K., Snyder, J. T., Siderovski, D. P., Campbell, S. L. & Sondek, J. (2002). *EMBO J.* **21**, 1315–1326.
Schmidt, A. & Hall, A. (2002). *Genes Dev.* **16**, 1587–1609.
Snyder, J. T., Worthylake, D. K., Rossman, K. L., Betts, L., Pruitt, W. M., Siderovski, D. P., Der, C. J. & Sondek, J. (2002). *Nature Struct. Biol.* **9**, 468–475.
Vagin, A. & Teplyakov, A. (1997). *J. Appl. Cryst.* **30**, 1022–1025.
Wells, C. D., Gutowski, S., Bollag, G. & Sternweis, P. C. (2001). *J. Biol. Chem.* **276**, 28897–28905.
Wells, C. D., Liu, M. Y., Jackson, M., Gutowski, S., Sternweis, P. M., Rothstein, J. D., Kozasa, T. & Sternweis, P. C. (2002). *J. Biol. Chem.* **277**, 1174–1181.
Worthylake, D. K., Rossman, K. L. & Sondek, J. (2000). *Nature (London)*, **408**, 682–688.